



MiniSShot trajectory study

Rev. 20091115

Overview

This is an overview of the trajectory and dynamics for the MiniSShot vehicle.

Aerodynamic drag and stability is investigated for the entire MiniSShot flight.

The trajectory is calculated for the nominal conditions, and its sensitivity towards changes in:

- Launch tower elevation angle.
- Phase 2 ignition timing.
- Drag coefficient.
- Dry mass.
- Launch tower length.
- Surface wind.

is investigated.

Except when noted, all calculations are performed using the authors own software “Launch” for trajectory simulations and “Aerolab” for aerodynamic properties. Furthermore, the Rogers Aerospace “RasAero” has been used to gather 2'nd opinions for trajectory results and stability.

The nature of the vehicle makes both stability and trajectory analysis somewhat tricky, and the intention of this report is to provide sufficient information for proper range safety and recovery despite the uncertainties.

The overall conclusion is that the MiniSShot vehicle will reach an altitude somewhere between 12 and 15 kilometers, and that post flight data analysis will be important for improving the predictions of the performance of the follow up projects.

Table of Contents

Vehicle overview.....	4
MiniSShot parts list.....	6
MiniSShot stability analysis.....	13
MiniSShot cd analysis.....	16
Trajectory analysis.....	18
Launch tower elevation angle.....	18
Phase 2 ignition timing.....	20
Coefficient of drag.....	21
Dry mass.....	21
Launch tower length.....	22
Supplemental calculations.....	23
Drag and stability.....	23
Wind sensitivity.....	25

Vehicle overview

The vehicle layout can be seen below. It has a quite long 34:1 body fineness with a 5.5:1 $3/4$ power shaped nose cone and 4 clipped delta fins. The fin semi span is approximately 110% of the body diameter. The rocket body has a diameter of 89mm, but with some sections slightly wider (90mm). A set of camera fairings are positioned at approximately one 3rd of the body length from the nose cone apex. The camera fairings are modeled as a set of canards, reducing the vehicle stability around the Y-axis of the vehicle but not around the Z-axis.

MiniSShot parts list

The vehicle parts have been modeled according to the “Iteration 2” 2009-09-13 vehicle mass statement. The vehicle parts are modeled using approximate shapes with locations and densities adjusted to match the specified masses and stations. This means that the model parts will be similar but not identical to their real counterparts, but close enough to give a usable indication of the overall vehicle dynamics.

The (model) parts list for the MiniSShot rocket is shown below. All CG stations are measured from the nose cone apex. The roll inertial moments are referenced around the rocket center axis and the pitch inertial moments are referenced around the nose cone apex.

Part No.	Designation	Mass	Type	CG	Pitch Inertial Moment	Roll Inertial Moment
		<i>(kg)</i>		<i>(mm)</i>	<i>(kg*m²)</i>	<i>(kg*m²)</i>
1	Nozzle outer divergent part	0.0874	Fixed	3167.5085	0.87712	0.0000385
2	Nozzle inner divergent part	-0.0788	Fixed	3168.3571	-0.79105	-0.0000321
3	Nozzle outer convergent part	3.0281	Fixed	3093.5000	28.98078	0.0029982
4	Nozzle inner convergent part	-1.4559	Fixed	3086.2790	-13.86832	-0.0008381
5	Nozzle detail	-0.6669	Fixed	3113.5000	-6.46499	-0.0009604
6	Aft casing	1.1180	Fixed	2633.0000	7.82652	0.0021167
7	Mid bulkhead	0.5060	Fixed	2144.0000	2.32646	0.0006704
8	Forward bulkhead	0.2140	Fixed	1235.0000	0.32656	0.0002119
9	Forward casing	1.0930	Fixed	1662.0000	3.10076	0.0020694
10	Aft casting tubes	0.7231	Fixed	2637.0000	5.06107	0.0012163

Part No.	Designation	Mass	Type	CG	Pitch Inertial Moment	Roll Inertial Moment
		<i>(kg)</i>		<i>(mm)</i>	<i>(kg*m²)</i>	<i>(kg*m²)</i>
11	Forward casting tubes	0.6333	Fixed	1671.0000	1.80203	0.0010652
12	Aft thermal barrier	0.0935	Fixed	2637.0000	0.65017	0.0001770
13	Forward thermal barrier	0.0914	Fixed	1662.0000	0.25263	0.0001730
14	Closure attachment screws, nozzle	0.0274	Fixed	3093.0000	0.26239	0.0000531
15	Closure attachment screws, mid bulkhead	0.0547	Fixed	2143.0000	0.25109	0.0001035
16	Closure attachment screws, fwd bulkhead	0.0274	Fixed	1220.0000	0.04085	0.0000531
17	Igniter	0.0200	Fixed	1272.0000	0.03237	0.0000002
18	Aft Avionics Fairing	0.1030	Fixed	1051.0000	0.11452	0.0001950
19	Recovery compartment fairing	0.1270	Fixed	745.0000	0.07251	0.0002404
20	Fins	0.2200	Fixed	2956.0000	1.92259	0.0014992
21	Motor coupler	0.0410	Fixed	1180.0000	0.05707	0.0000370
22	Aft tapered coupler	0.0370	Fixed	928.0000	0.03188	0.0000296
23	Forward tapered coupler	0.0350	Fixed	911.5000	0.02908	0.0000280
24	Nosecone coupler	0.0580	Fixed	561.0000	0.01828	0.0000524
25	Pyro separation link	0.0500	Fixed	919.5000	0.04229	0.0000025

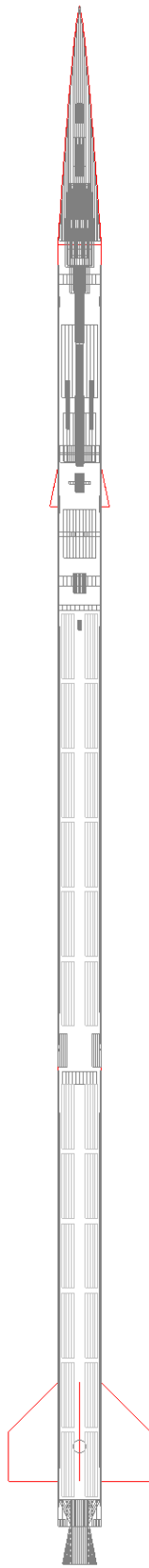
Part No.	Designation	Mass	Type	CG	Pitch Inertial Moment	Roll Inertial Moment
		<i>(kg)</i>		<i>(mm)</i>	<i>(kg*m²)</i>	<i>(kg*m²)</i>
26	Aiptek camera	0.1860	Fixed	1084.0000	0.21875	0.0000982
27	Aiptek camera support	0.0400	Fixed	1084.0000	0.04705	0.0000362
28	Capsule Recovery beacon + Amp	0.0752	Fixed	979.0000	0.07210	0.0000038
29	Capsule Recovery beacon & amp batteries	0.0807	Fixed	979.0000	0.07731	0.0000040
30	Recovery beacon supports	0.0300	Fixed	979.0000	0.02878	0.0000076
31	Booster Recovery beacon + Amp	0.0752	Fixed	221.0000	0.00369	0.0000038
32	Booster Recovery beacon/ amp batteries	0.0807	Fixed	221.0000	0.00396	0.0000040
33	Drogue chutes	0.0820	Fixed	886.0000	0.06443	0.0000433
34	Main parachute	0.0580	Fixed	730.0000	0.03104	0.0000397
35	Drogue tether	0.1160	Fixed	850.0000	0.08392	0.0000058
36	Main tether	0.0580	Fixed	617.0000	0.02218	0.0000029
37	Pyro Release Device + fittings	0.1000	Fixed	607.0000	0.03695	0.0001791
38	Main computer	0.0500	Fixed	403.0000	0.00814	0.0000100
39	Chute Controller	0.0400	Fixed	562.0000	0.01265	0.0000080

Part No.	Designation	Mass	Type	CG	Pitch Inertial Moment	Roll Inertial Moment
		<i>(kg)</i>		<i>(mm)</i>	<i>(kg*m²)</i>	<i>(kg*m²)</i>
40	TinyTrack	0.0340	Fixed	487.0000	0.00806	0.0000106
41	GPS unit	0.1020	Fixed	487.0000	0.02424	0.0000204
42	MiniATV unit	0.1700	Fixed	487.0000	0.04050	0.0000765
43	Nose cone	0.2400	Fixed	205.0000	0.01361	0.0002385
44	Avionics (fwd) support structure	0.0500	Fixed	457.0000	0.01053	0.0000156
45	thermal sensors	0.0147	Fixed	400.0000	0.00236	0.0000029
46	thermal board	0.0180	Fixed	210.0000	0.00079	0.0000002
47	vibration sensor	0.0200	Fixed	325.0000	0.00212	0.0000010
48	DTMF & GMRS receiver	0.0371	Fixed	300.0000	0.00335	0.0000029
49	Power supply, GMRS receiver	0.0300	Fixed	300.0000	0.00270	0.0000015
50	Power supply, MC	0.0600	Fixed	400.0000	0.00962	0.0000068
51	Power supply, CC	0.0600	Fixed	562.0000	0.01898	0.0000047
52	Power supply, telemetry	0.1000	Fixed	487.0000	0.02375	0.0000153
53	Pressure transducer	0.0750	Fixed	1185.0000	0.10534	0.0000059
54	tether anchor fitting	0.0500	Fixed	1185.0000	0.07022	0.0000053
55	Delay plug	0.1740	Fixed	2200.0000	0.84222	0.0001096
56	FeatherWeight Altimeter	0.0111	Fixed	562.0000	0.00349	0.0000006
57	FeatherWeight power supply	0.0150	Fixed	562.0000	0.00475	0.0000004

Part No.	Designation	Mass	Type	CG	Pitch Inertial Moment	Roll Inertial Moment
		<i>(kg)</i>		<i>(mm)</i>	<i>(kg*m²)</i>	<i>(kg*m²)</i>
58	Camera mirror & fairings	0.0250	Fixed	1023.0000	0.02615	0.0000447
59	Wiring	0.1000	Fixed	820.0000	0.06778	0.0000028
60	Miscellaneous	0.1500	Fixed	820.0000	0.10101	0.0000867
61	Forward propellant segment 1	0.8750	Propellant	1314.4000	1.51335	0.0006682
62	Forward propellant segment 2	0.8750	Propellant	1457.0400	1.85926	0.0006682
63	Forward propellant segment 3	0.8750	Propellant	1599.6800	2.24077	0.0006682
64	Forward propellant segment 4	0.8750	Propellant	1742.3200	2.65784	0.0006682
65	Forward propellant segment 5	0.8750	Propellant	1884.9600	3.11056	0.0006682
66	Forward propellant segment 6	0.8750	Propellant	2027.6000	3.59889	0.0006682
67	Aft propellant segment 1	0.8750	Propellant	2280.4000	4.55191	0.0006682
68	Aft propellant segment 2	0.8750	Propellant	2423.0400	5.13896	0.0006682
69	Aft propellant segment 3	0.8750	Propellant	2565.6800	5.76162	0.0006682
70	Aft propellant segment 4	0.8750	Propellant	2708.3200	6.41988	0.0006682
71	Aft propellant segment 5	0.8750	Propellant	2850.9600	7.11374	0.0006682
72	Aft propellant segment 6	0.8750	Propellant	2993.6000	7.84322	0.0006682

	Weight	CG	Pitch Inertial Moment	Roll Inertial Moment
	<i>(kg)</i>	<i>(mm)</i>	<i>(kg*m²)</i>	<i>(kg*m²)</i>
Complete Rocket	19.2945	1978.6221	86.85716	0.0203175
Phase 1 burnout	14.0444	1732.5074	50.02772	0.0163084
Phase 2 ignition	13.8704	1726.6419	49.18561	0.0161988
Empty rocket	8.6204	1760.5306	34.20494	0.0121897

A sketch of the MiniSShot vehicle cross section with the model parts visible is shown below.



MiniSShot stability analysis

The stability calculation is performed for the MiniSShot vehicle, assuming the mass distribution of the modeled parts, and a set of 4 camera fairing “canards”. The camera fairings are to be cut from tubes, but they are modeled as planar fins with a sharp leading edge. The root thickness of the fin is only half the root thickness of the real fairing due to thickness limitations in the aerodynamic model. It is possible that the predicted lift on the planar fin will exceed the lift on the rounded camera fairing, but the planar fin will give a conservative stability margin. In reality, there are only 2 camera fairings, giving the rocket asymmetric stability characteristics. The 4-canard vehicle model gives the stability margin around the axis of least stability.

The stability analysis is performed using the Barrowman method, the cardboard cutout method and the method of the NACA TN1307 - of which Barrowmans method is a subset valid for velocities up to approximately Mach 0.5.

The stability analysis is split into 3 parts:

- Phase 1 static stability.
- Phase 2 static stability.
- Liftoff stability.

A preliminary trajectory analysis has determined the approximate velocity range for boost and coast for both phases, and the approximate CG location during the boost phases has been calculated accordingly.

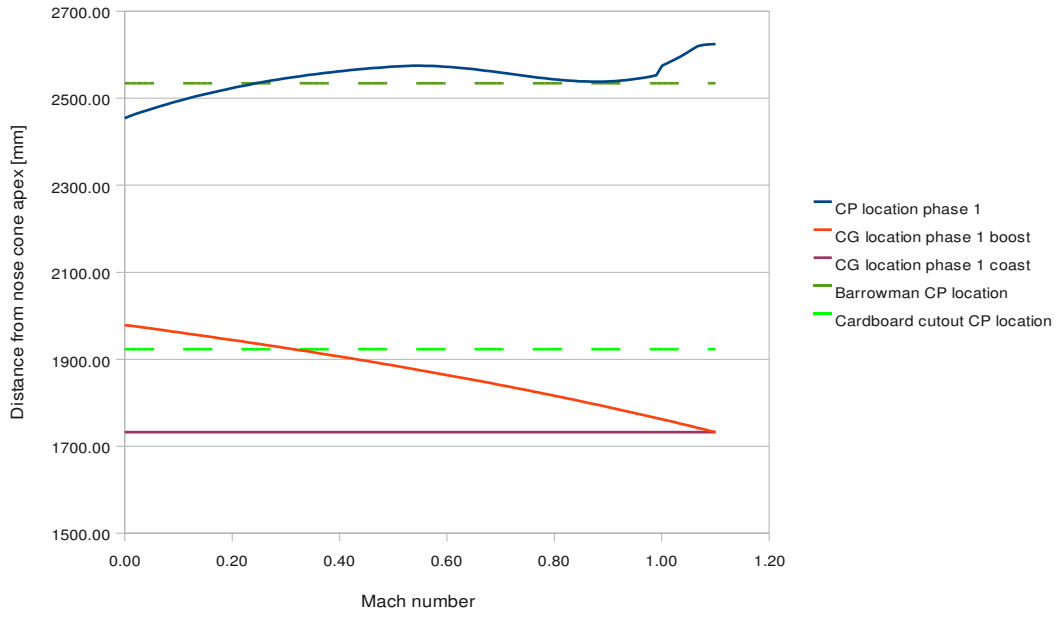
During phase 1, the vehicle accelerates from zero to approximately Mach 1.1 and decelerates back to Mach 0.5. Stability margin is shown for zero to Mach 1.1 during phase 1 burn and back to zero for the subsequent coast phase.

During phase 2, the vehicle accelerates from approximately Mach 0.5 to Mach 2.2, before it coasts back to almost zero. Stability margin is indicated from zero to Mach 4.

Note that the velocity ranges will depend on the final version of the vehicle, and could deviate somewhat from the numbers used for this analysis. This is however not a problem since the stability margin is generous.

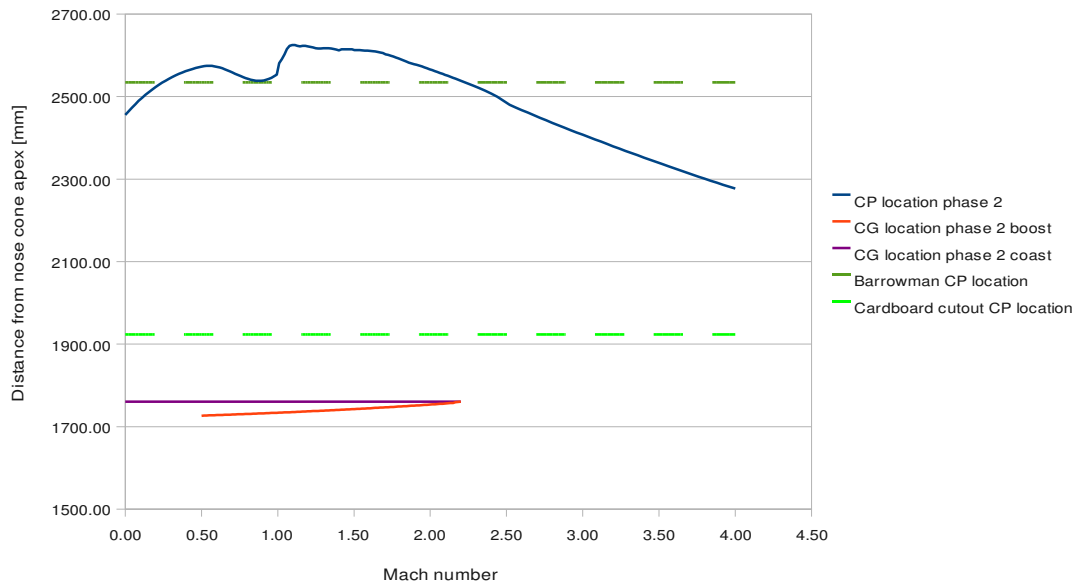
MiniSShot static stability

Phase 1 boost and coast



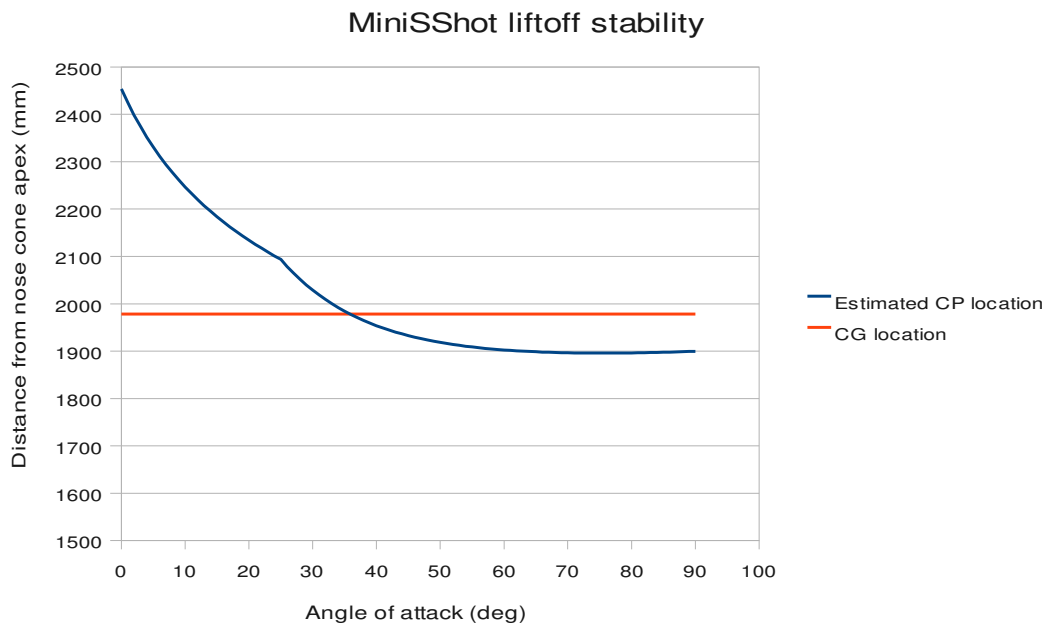
MiniSShot static stability

Phase 2 boost and coast



The static stability is ensured by a margin of more than 5 calipers during the entire flight, with the minimum stability margin at liftoff.

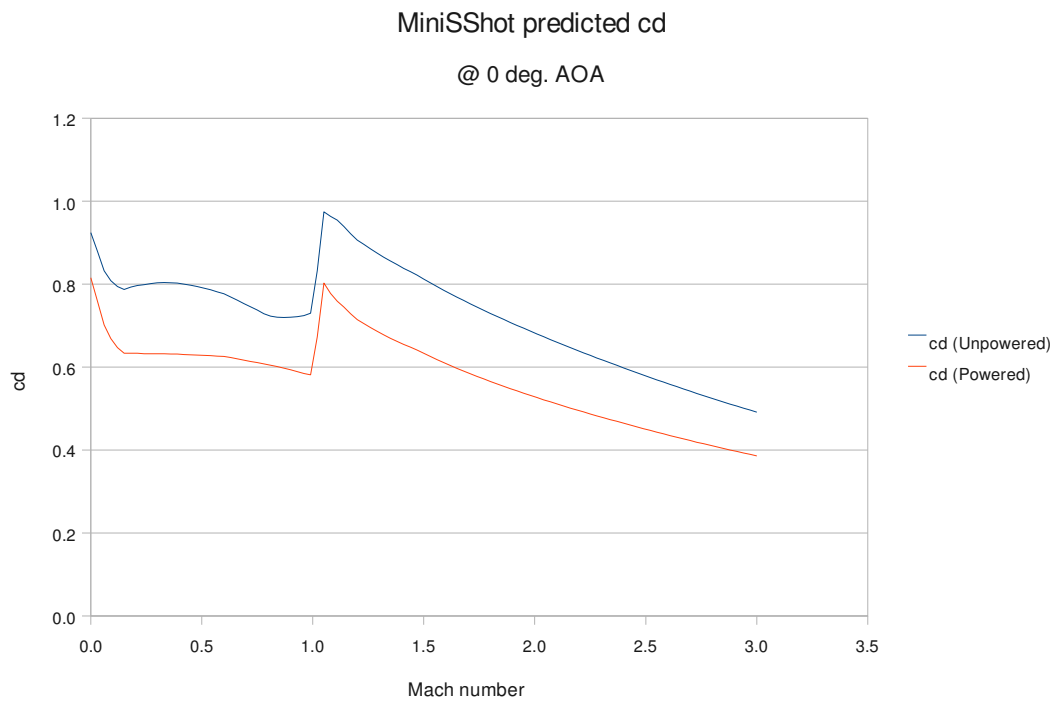
The cardboard cutout calculation is a simplified 90 degree AOA CP estimate. The stability calculations reveal that the vehicle is almost stable, even according to the cardboard cutout method. A more detailed analysis predicts however, that the vehicle will become unstable at approximately 39 degrees AOA.



For a 4.3m launch tower, the predicted velocity is 29.8m/s at the end of the tower, and a neutral stability at 39 degrees AOA corresponds to a limiting case surface wind of 24m/s.

Even though the MiniSShot vehicle may be stable at quite high surface winds, the large stability margin will make it prone to weathercocking, and due to the nature of the trajectory of a dual phase rocket powered vehicle, calm conditions at launch will be critical for ensuring a successful launch.

At the time of the calculations, the use of a launch tower or rail has not been made, and the cd calculation does not include launch lugs.



The cd predictions cover the entire flight of the vehicle. The coasting phase between phase 1 burnout and phase 2 ignition is however neither powered nor unpowered, but something in between, as the delay plug will produce some amount of exhaust gases.

Trajectory analysis

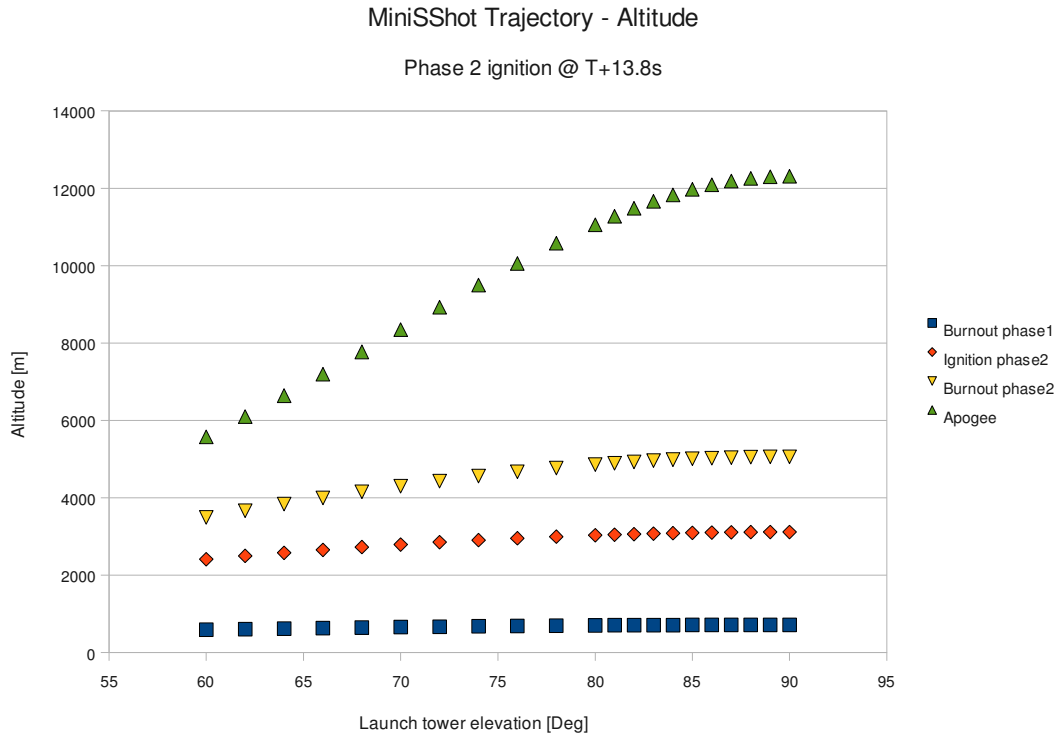
The MiniSShot trajectory has been modeled as that of a 2 stage vehicle, assuming the mass of the delay plug as the dry mass of the first stage. Phase 1 and phase 2 thrust is treated as two separate motors to allow simulations of different phase 2 ignition timings. Measured thrust data from the ProtoSShot 3 static test are used for simulating the burn(s), and the trajectory simulations invokes the predicted drag data for the highest fidelity. For simplicity, the first stage is always dropped at T+13.8 seconds (10 seconds after phase 1 burnout), regardless of the phase 2 ignition timing. A total dry mass of 19.26kg is assumed according to the parts list.

The launch site is assumed to be located at 575 meters above sea level, and a 4.3 meter launch tower is assumed, except where otherwise noted. The calculations are terminated at apogee - recovery considered outside the scope of this analysis.

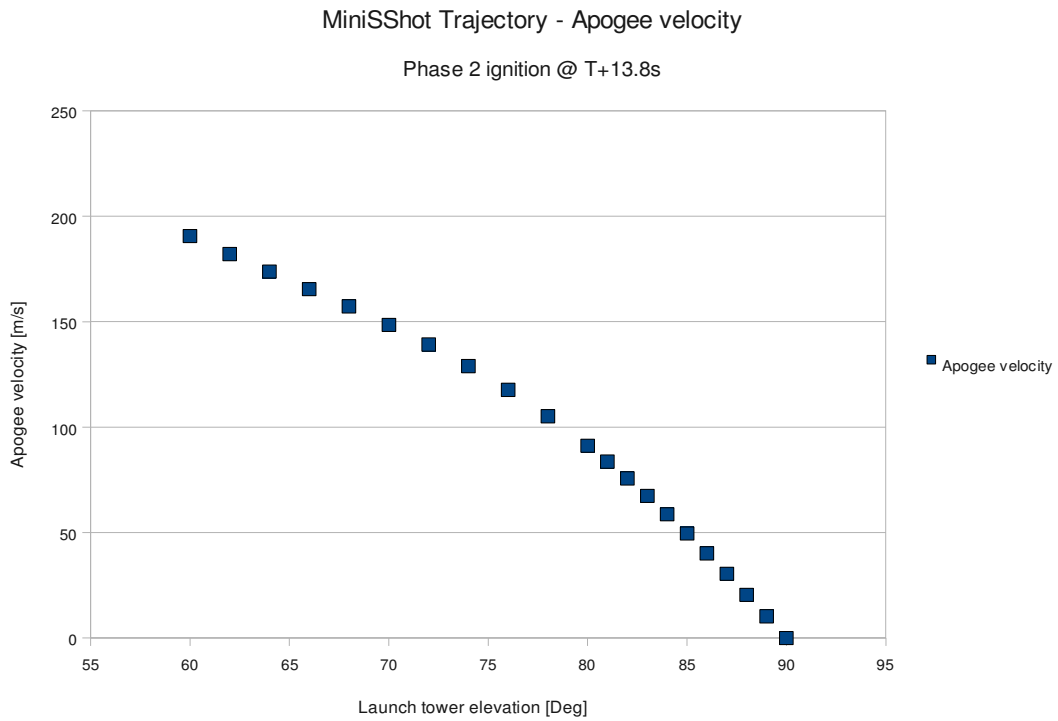
Since a number of yet unknown factors affect the trajectory of the MiniSShot vehicle, the following simulations are not to be considered final and square, but rather it is a catalog of simulations that describes the overall characteristics of the trajectory and its sensitivities with respect to certain parameters.

Launch tower elevation angle

The MiniSShot trajectory has been calculated for launch tower elevation angles between 60 and 90 degrees, assuming that phase 2 ignition occurs at T+13.8s, corresponding to a 10 second delay between phase 1 burnout and phase 2 ignition. The gravity turn at 60 degrees is significant, causing the vehicle to lose more than half its potential apogee altitude. At nominal conditions (85 degrees), gravity turn only has a slight impact on the summit altitude. However, surface winds at the launch site could potentially cause the vehicle to ascend at a less vertical trajectory than expected.

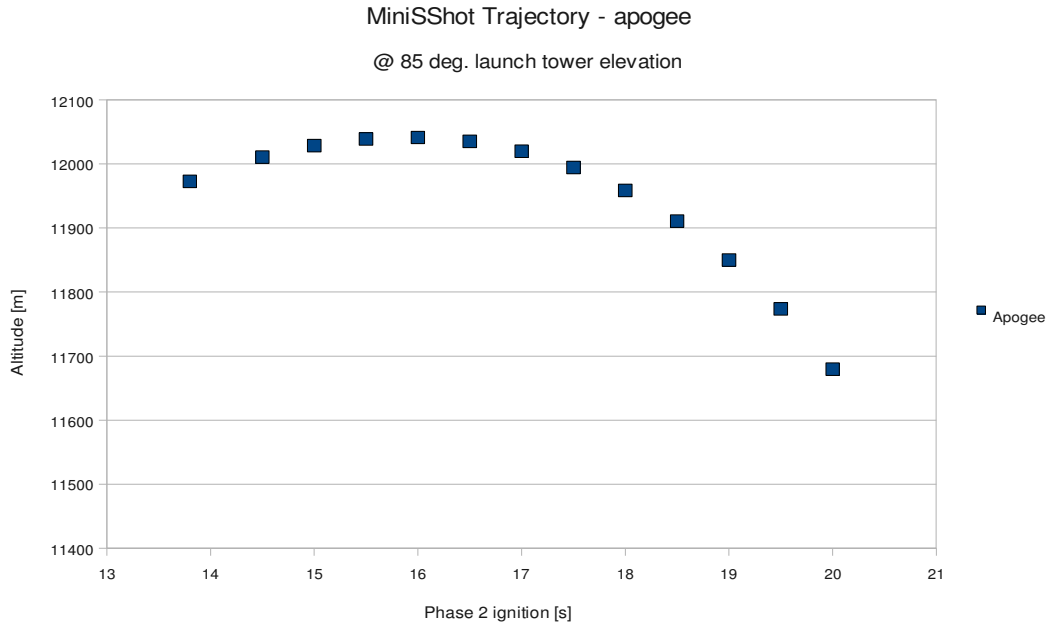


The launch tower elevation angle also affects the velocity at apogee. The pilot chute must be able to handle release velocities of 50-150m/s.

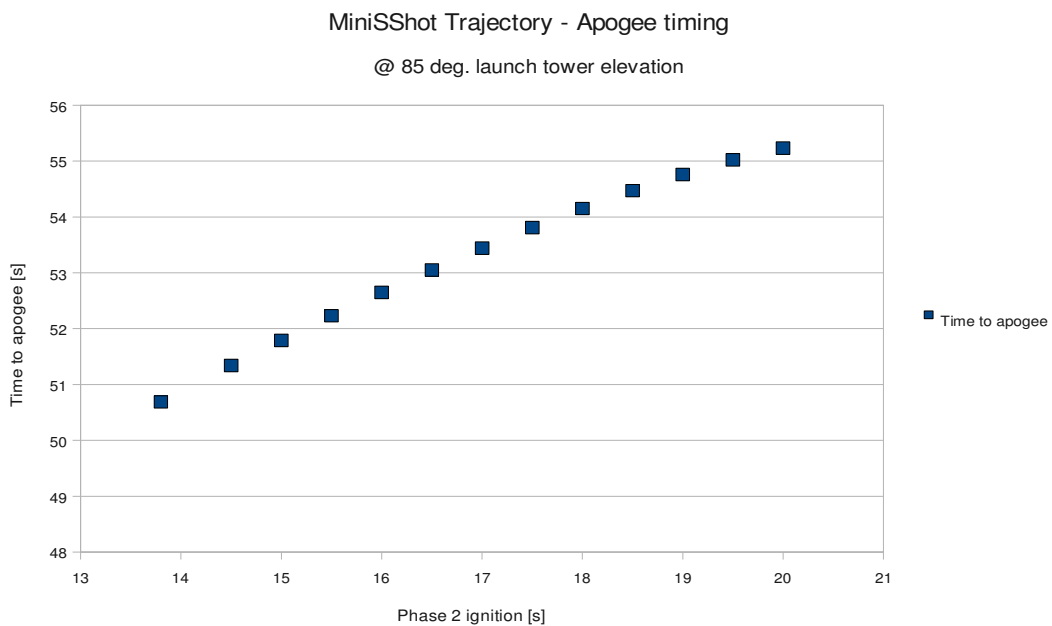


Phase 2 ignition timing

The summit altitude depends on the phase 2 ignition. The optimal phase 2 ignition occurs at approximately T+16 s.



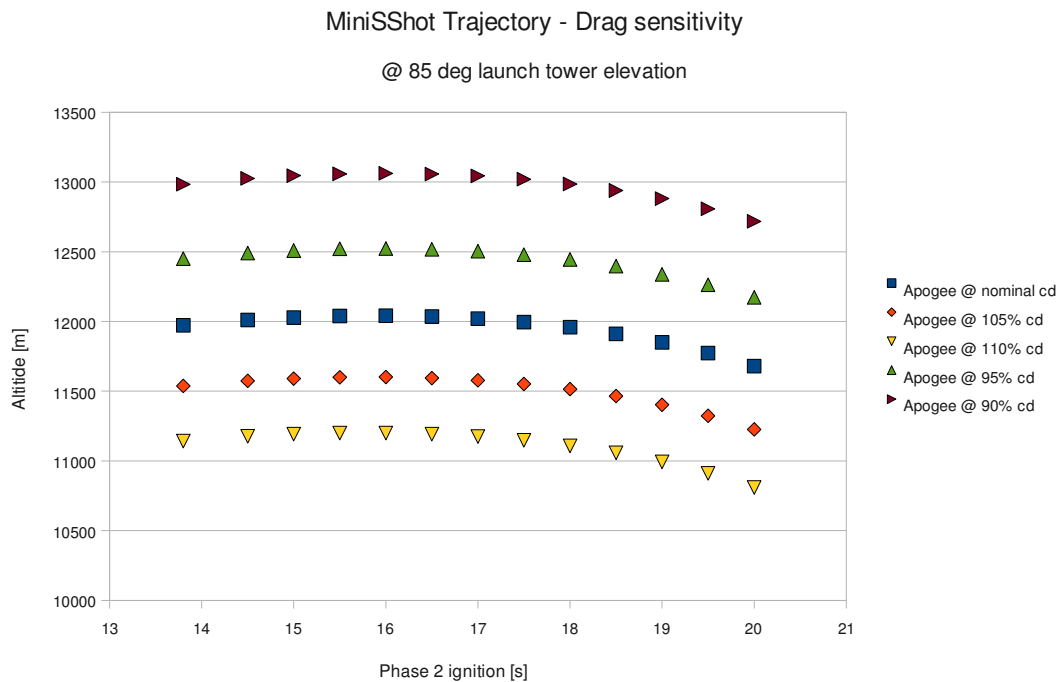
Phase 2 ignition also affects the time to apogee:



Despite T+16s being the optimum for phase 2 ignition, the ignition pulse should occur 1-2 seconds earlier to counter any ignition delay. A slightly early ignition is much better than a late ignition.

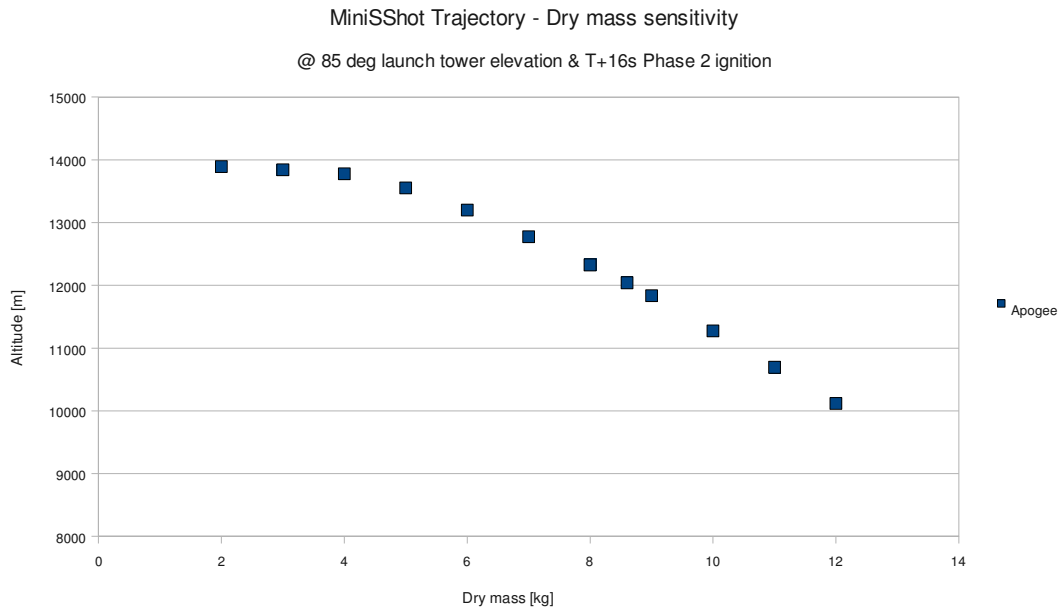
Coefficient of drag

The drag coefficient has a large impact on the apogee. This is severe since the uneven body tube makes the actual drag coefficient hard to predict. A 1% change of the drag coefficient corresponds roughly to 100 meters at apogee. Note that any coning motion during the ascent will change (increase) the drag coefficient. Note also, that the optimal phase 2 ignition remains unchanged at T+16 s.



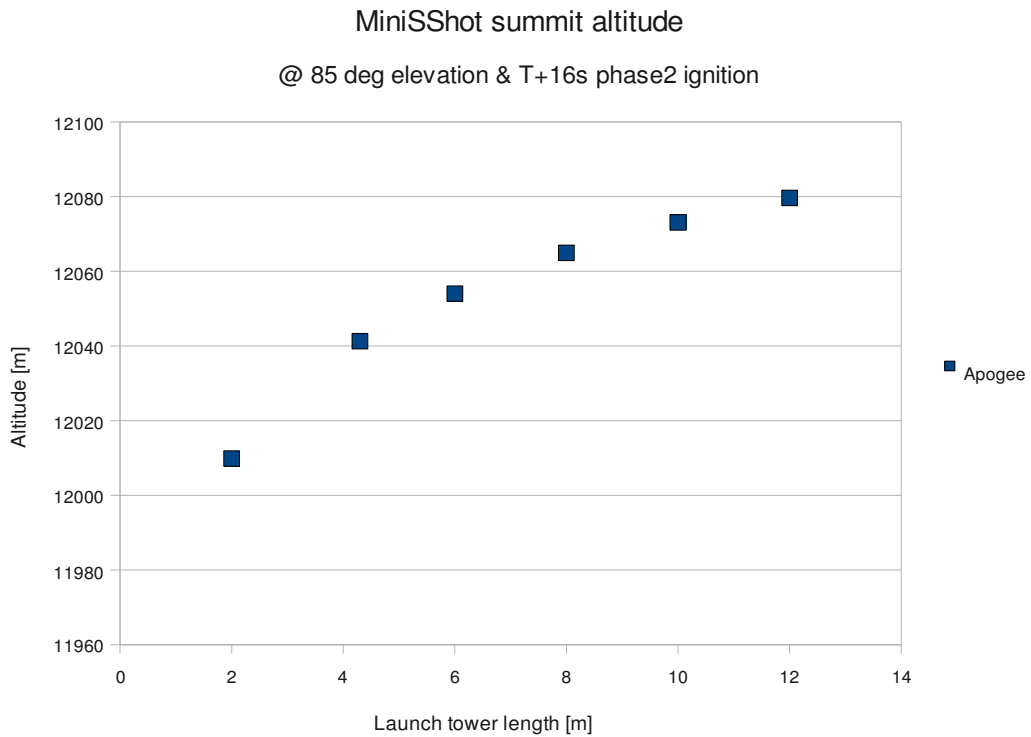
Dry mass

The dry mass sensitivity chart reveals - as expected - that any reduction in the dry mass will result in a higher apogee. The dual phase concept makes dry mass optimization trivial as it reduces drag losses significantly.



Launch tower length

The length of the launch tower has yet to be decided. It does have a slight impact on the apogee, although it is of secondary importance.



Supplemental calculations

A number of supplemental calculations has been performed using the Rogers Aerospace “RasAero” software. Results are not directly comparable to those of the previous chapters for the following reasons:

- RasAero allows only one set of fins. As a result, the c_d value will be lower and stability margin will be higher than those of the previous simulations.
- RasAero allows only single stage rockets. As a result, only the case of phase 2 ignition at T+13.8 seconds is covered. This also affects the drag of the rocket, since the drag model for powered flight is invoked from liftoff until phase 2 burnout. As a consequence, RasAero will give more optimistic predictions, than those of the previous simulations.
- RasAero does not allow for power series nose cones. Instead, the nose cone is modeled as a slightly rounded cone. This is likely to be of secondary importance.

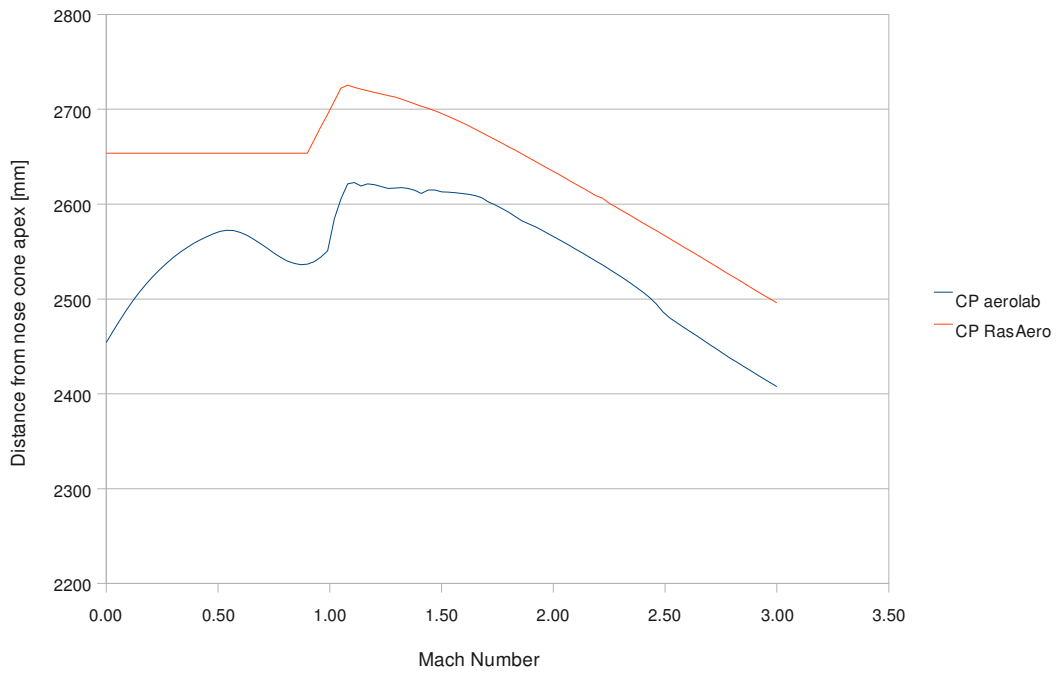
Despite the differences, RasAero simulations will be able to sanity check Launch simulations and vice versa. The differences in c_d values are biggest at subsonic speeds. This primarily affects the drag losses during the inter phase coasting and the velocity at phase 2 ignition. Furthermore, the use of unpowered c_d values at the inter-phase coasting will make Launch predict the lower bounds of the expected trajectory, while the lower c_d values will make RasAero predict the upper bounds.

Drag and stability

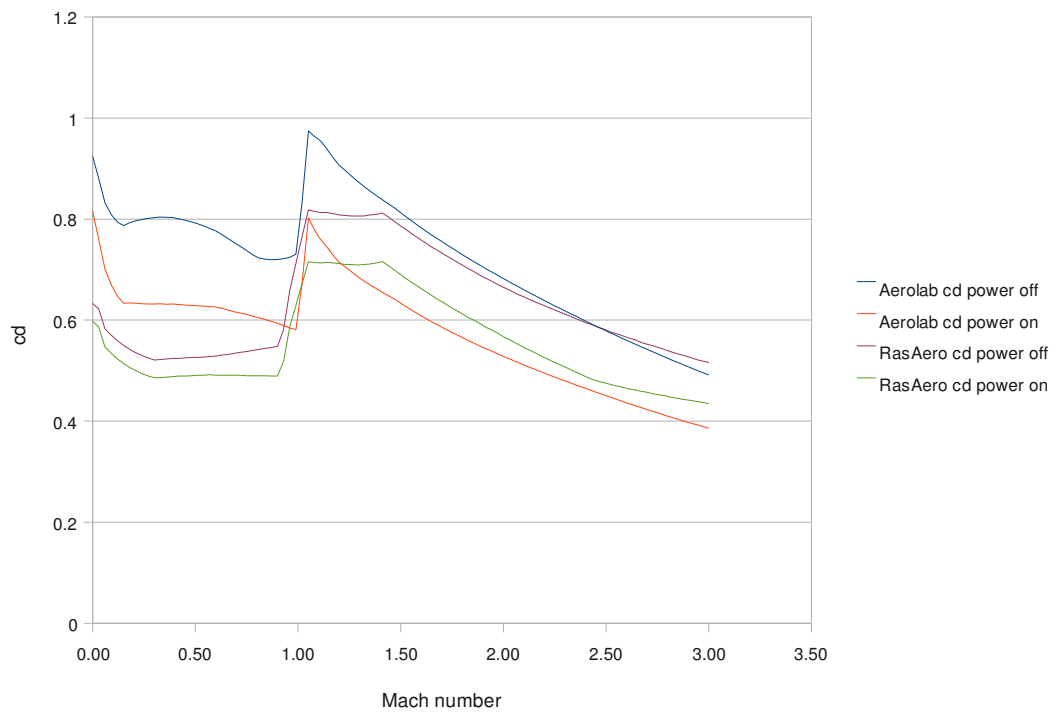
Comparing the stability calculations reveals - as expected - a nearly constant difference of the vehicle CP location at supersonic speeds, originating from the camera fairing not being included in the RasAero model. At sub and transonic speeds there are additional differences indicating that the RasAero employs a somewhat simpler model.

The drag prediction made by RasAero is somewhat more favorable at subsonic and transonic speeds than the values predicted by Aerolab. The reason for this difference is not known in details. At supersonic speeds, there is a quite good agreement between the two softwares.

MiniSShot CP location @ 0 deg AOA



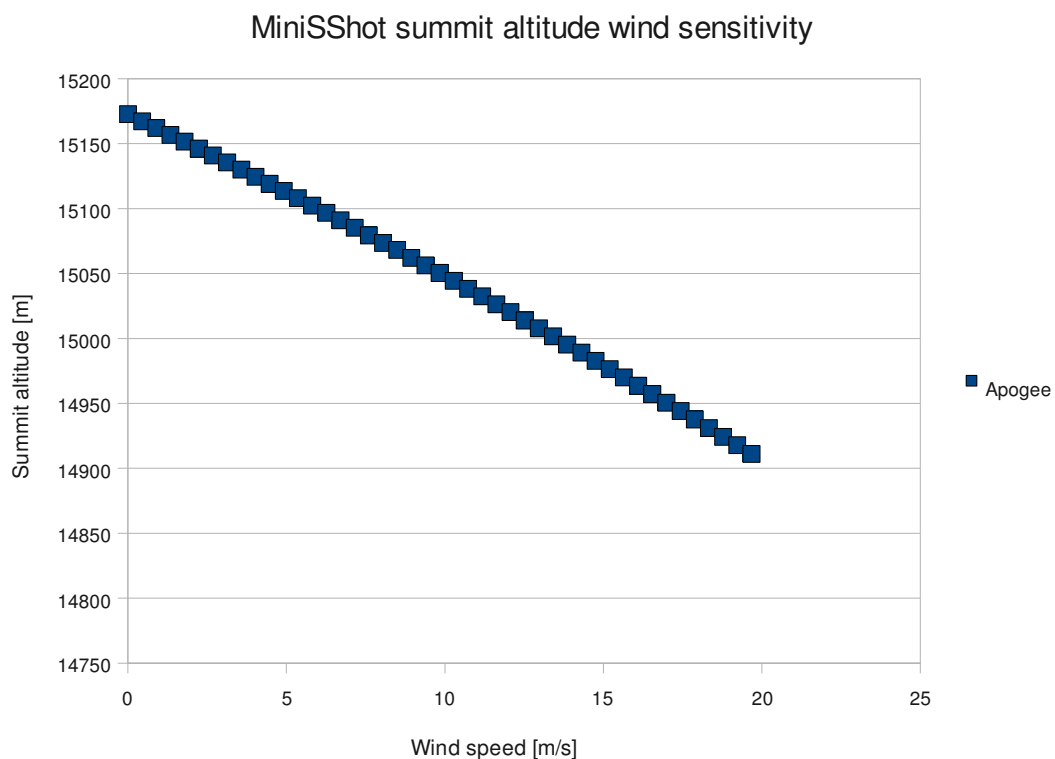
MiniSShot cd @ 0 deg AOA



The lower c_d values combined with longer operation in “power on” mode makes RasAero altitude predictions are roughly 25% more optimistic than the ones made by Aerolab. This is in good agreement with the previously noted sensitivity against drag variations. The truth is likely to be somewhere in between the predictions as the “power on” condition between first and second phase is likely to be partially true.

Wind sensitivity

The RasAero software has been used to predict the sensitivity against surface wind. The surface wind will affect the apparent launch elevation angle, and thereby the summit altitude.



The surface wind sensitivity is surprisingly low considering the large stability margin in lift-off. The fast acceleration and fairly high inertial moment is of good help in this situation. It is not clear if the wind model compensates for altitude effects, and some additional influence of the surface winds at the second phase ignition must be anticipated.